Simulating Fast Timing Cherenkov Detectors

Moriah Tobin
Office of Science, Science Undergraduate Laboratory Internships (SULI) Program

Reed College, Portland

Fermi National Accelerator Laboratory
Batavia, Illinois

August 9, 2010

Prepared in partial fulfillment of the requirement of the Office of Science, Department of Energy's Science Undergraduate Laboratory Internships (SULI) Program under the direction of Michael G. Albrow in the Particle Physics Division at Fermi National Accelerator Laboratory.

Participant: ___________________________________
Signature

Research Advisor: ___________________________________
Signature

ABSTRACT

Optimization of Cherenkov Detectors for Fast Timing
Moriah Tobin (Reed College, Portland, OR 97202), Mike Albrow (Fermi National Accelerator Laboratory, Batavia, IL 60510).

As we continue to push the frontiers of accelerator design, we open up the possibility of observing more energetic particle interactions. However, observation of these interactions requires incredibly precise and accurate measurements. At the forefront lies the Large Hadron Collider (LHC), which will collide two 7 TeV proton beams. A proposed addition to the Compact Muon Solenoid experiment at the LHC, the high precision spectrometer (HPS), will probe interactions in which two protons scatter off of each other at very small angles, correlating to a small (< 5%) fractional loss of momentum. This process will look deeply into particle interactions and may expose new physics, including Higgs boson production and events outside of the Standard Model. To identify the scattering vertex, and thus determine which protons were involved in the same scattering events, the proton detectors must have a timing resolution on the order of picoseconds. Cherenkov detectors have been experimentally shown to have timing resolutions as low as 15 ps, which could be optimized through simulation. This study models quartz Cherenkov detectors to find the optimal configuration for producing the best timing resolution. The study used two programming languages based on C++: Geant4 to model the passage of particles in matter, and ROOT for analysis and modeling the photodetector. The simulation predicts the timing resolution of a quartz radiator leading to a silicon photomultiplier (SiPM) in the beamline to be a few picoseconds. However, this study has not yet been able to replicate the experimental data. The simulated number of photoelectrons in the detector was consistently higher than the experimentally measured value. An experimental study would be needed to determine whether this loss of photoelectrons occurs in the quartz crystal, at the interface of the crystal with the photodetector, or at the photodetector itself. The simulated timing resolution has also been consistently better than the experimental value by a factor of two to five, accounting for the electronics, which have a timing resolution of 3-4 ps. Nevertheless, the study indicates that Cherenkov detectors are an excellent choice for fast timing detectors, though further investigation needs to be done to confirm the causes of the inefficiencies in the actual detector.

INTRODUCTION

The Large Hadron Collider (LHC) is exploring many regions of particle interactions never before accessible. One process that holds particular interest is central exclusion production (CEP). In CEP, two protons scatter at small angles and produce a new particle, as shown in Figure 1. This process is capable of producing the Higgs boson at the LHC for the current predicted masses of the Higgs (~100-200 GeV/c^2), and could also produce particles outside the Standard Model. Measuring this process would allow for fine mass measurements of the produced particle, as well as quantum number determination, and in-depth studies of quantum chromodynamics (QCD) [1].

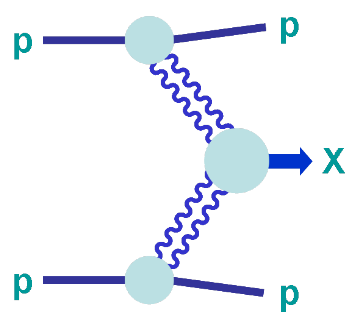

Figure 1: Proton-proton scattering resulting in the production of a new particle (X) through a process known as CEP (http://www.hep.phy.cam.ac.uk/theory/research/cep.html).

To measure this process, the High Precision Spectrometer (HPS) has been proposed. The HPS would situate a detector in the high dispersion region at 420 m on both sides of the collision point in CMS to detect scattered protons [2]. To determine the interaction position of these protons along the beam line to 2.1 mm requires a timing resolution of 10 ps in the detector. This level of accuracy is needed to reduce background events to a manageable level [1].

10 ps is the time it takes for light to travel approximately 3 mm through a vacuum; this must be taken into account when designing a timing detector for the HPS project. Cherenkov radiation is an excellent choice because it is a prompt effect, whereas scintillation is a slower

process. When a charged particle travels through a dielectric medium at a speed greater than the speed of light for that medium, the electric field of the particle excites the medium's electrons, which then emit photons to return to their lowest energy state. These emitted photons constructively interfere and produce a cone of light produced about the particle's line of flight at the Cherenkov angle, as shown in Figure 2, and are called primary photons. This process in electromagnetism is analogous to the production of a sonic boom by supersonic airplanes for longitudinal waves. The proton can also collide with electrons in the material, causing them to travel at relativistic speeds for a short distance (these electrons are called delta rays or delta electrons), creating more Cherenkov photons, referred to as secondary photons.

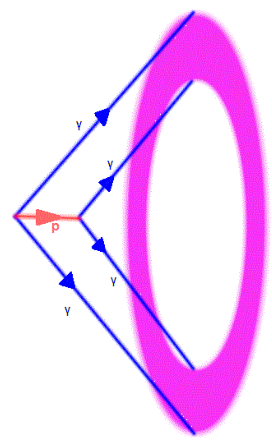

Figure 2: Depiction of Cherenkov radiation in a crystal. The red line is the charged particle trajectory, the blue lines are photons emitted at the Cherenkov angle, and the pink circle shows the pattern the cone of light makes incident upon a surface (http://www.ps.uci.edu/~superk/superk_detector.html).

Cherenkov detectors have been shown to have timing resolutions as low as 6.2 ps [2]. However, the HPS requires edgeless detectors with a timing resolution of 10 ps. Edgeless Cherenkov detectors have produced timing resolutions as low as 15 ps [3]. This indicates that edgeless Cherenkov detectors could be optimized to yield 10 ps timing resolutions for HPS. This study produced a simulation for Cherenkov fast timing detectors to assist the design of an edgeless Cherenkov detector with a timing resolution of 10 ps or below.

MATERIALS AND METHODS

Geant4 is a C++-based Monte Carlo simulation program used to model particle interactions with matter. ROOT is a C++-based analysis program. In this study, Geant4 was used to simulate the interactions of the incident 7 TeV protons with the materials of the detector (including Rayleigh scattering, boundary processes, absorption, and Cherenkov emission), while ROOT was used as a framework to simulate the photodetector and for analysis.

Simulations were made for two different setups. First, 3 mm by 3 mm quartz bars of differing lengths (6, 10, 20 and 30 mm) were attached with optical grease to a photodetector, with the proton beam passing through the center of the quartz bar, as shown in Figure 3, called the SiPM setup. Secondly, a proton beam passing through 5mm by 5mm quartz bars of differing lengths at the Cherenkov angle of 48° from the axis of the quartz bar, as shown in Figure 4, referred to as the QUARtz TIming Cherenkov (QUARTIC) setup. Both of these setups had been tested in the beam line, allowing the simulations to be compared to data before extrapolation for optimization.

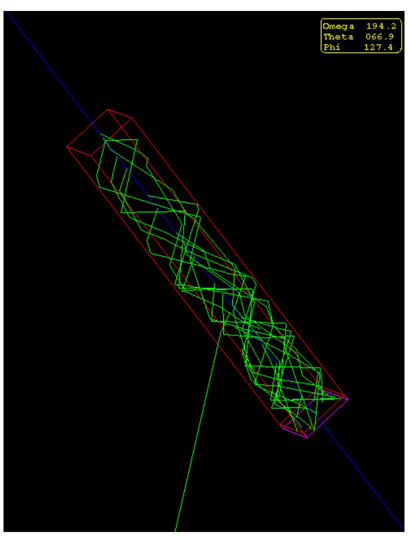

Figure 3: Setup for the SiPM simulations. The blue line is the proton trajectory, the red outlines the quartz crystal, the purple is the photodetector, and the green lines represent photon trajectories.

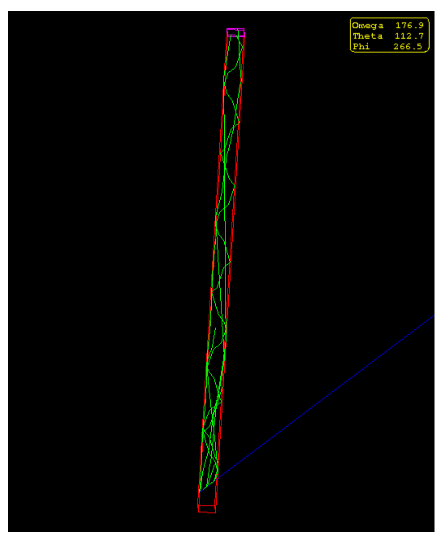

Figure 4: Setup for the QUARTIC simulations. The blue proton trajectory travels through the bar (outlined in red) at the Cherenkov angle, producing photons (green), some of which incident upon the photodetector (purple).

The study simulated two detectors. The first was the Hamamatsu 3 mm by 3 mm, ceramic-backed silicon photomultiplier (SiPM), a multi-pixel photon counter (MPPC) with 50 μm square pixels whose reported quantum efficiency is shown in Figure 5, along with a polynomial fit calculated in Excel and entered into the simulation to provide a smooth detector efficiency curve. The simulation used a time transit spread of 200 ps for the MPPC. In the simulation, we also lowered the MPPC efficiency by a constant factor to replicate the number of photoelectrons measured for the experimental setups. The second was the Hamamatsu MCP R3809U-65 with a time transit spread of 30 ps and quantum efficiency shown in Figure 6, also with the fit curve entered into the simulation.

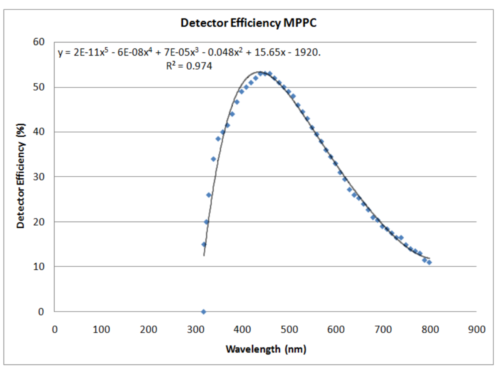

Figure 5: Detector efficiency curve for Hamamatsu MPPC, fit with a polynomial curve used as the detector efficiency in ROOT.

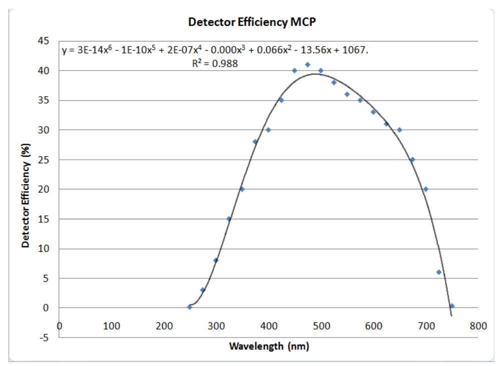

Figure 6: Detector efficiency curve for Hamamatsu MCP, fit with a polynomial curve used as the detector efficiency in ROOT.

Figure 7 shows the refractive index versus wavelength for quartz as used in the simulation. From this we see that the refractive index is much higher for blue-UV light than for red light where the photodetector's peak efficiency lies. The change in the refractive index also corresponds to a change in the Cherenkov angle for different emitted frequencies. However, the critical angle for reflection, on a surface parallel to the particle trajectory, is equal to the maximum Cherenkov angle. Hence, all the primary Cherenkov light in the quartz bar is totally internally reflected. There is a dispersion effect by which lower wavelength Cherenkov light arrives later, but is produced in greater quantities. We also did some preliminary studies with lead fluoride (PbF2), whose refractive index as a function of wavelength is shown in Figure 8.

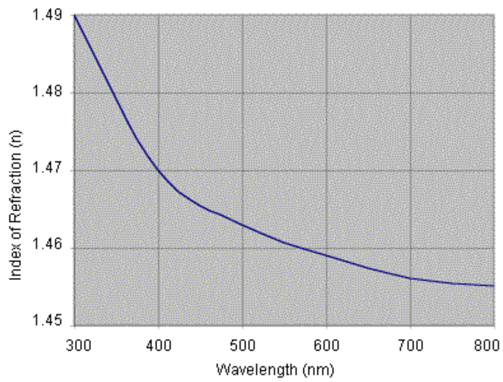

Figure 7: Refractive index of quartz (http://www.instant-analysis.com/Principles/spectra.htm).

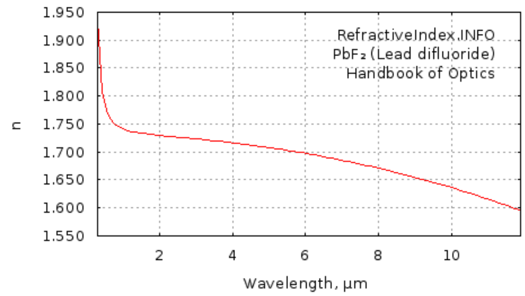

Figure 8: Refractive index of PbF2 (http://refractiveindex.info/?group=CRYSTALS&material=PbF2).

The experimental setup used a constant fraction discriminator (CFD) to measure the time of the pulse. To model this process, the simulated pulse was generated by pulling 100 times from a Gaussian with standard deviation equal to the time transit spread of the detector for each photoelectron produced in the detector then incorporating all of these times into a histogram. This step models the time transit spread of the detector, though to save computational time, we used a gain of 100 instead of the actual gain of 10^5-10^6. This histogram was then fit with a Gaussian and the time this Gaussian was at an inputted fraction of the peak height was the simulated time of detection. This accurately simulates the time transit spread of the MCP. However, it was recently discovered that this method of simulation is a poor model of the SiPM. This method artificially improves the timing resolution by improving photon statistics in the SiPM, and instead only one sample of the SiPM Gaussian should be used in further studies.

In the simulation, we inputted the properties of the materials and photodetectors used, and then ran a 7 TeV proton beam through the simulated environment. To get the timing resolution of the detector, we ran 1 000 protons through the detector and plotted the time of detection for each one in a histogram. The histogram was fit with a Gaussian and the standard deviation of the Gaussian was used for the timing resolution values.

RESULTS

The simulated photons reaching the detector arrived as expected. Figure 9 shows the number of photons of each wavelength reaching the detector, illustrating that Cherenkov radiation is primarily in the blue and UV. As the radiator bar length increases, the shape of the distribution remained constant, but the number of photons increased. Figure 10 shows the number of photons reaching the detector versus time, which is nearly constant with slight decrease until it decreases rapidly at a time difference of approximately the bar length, tailing off to zero, as well as the fraction of these photons that produce photoelectrons. Combining these two graphs in Figure 11, it is apparent that the later photons have shorter wavelengths.

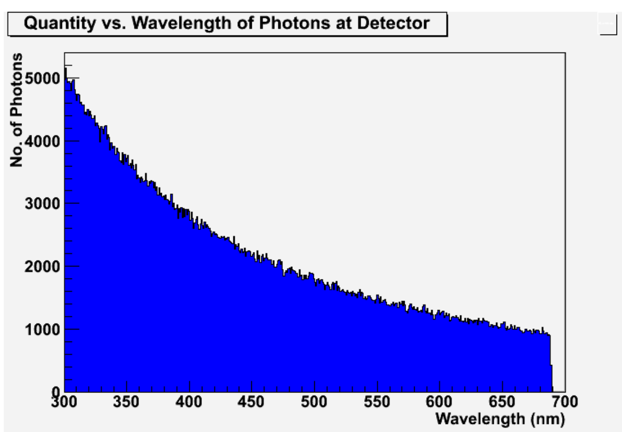

Figure 9: Photons incident upon photodetector as a function of wavelength.

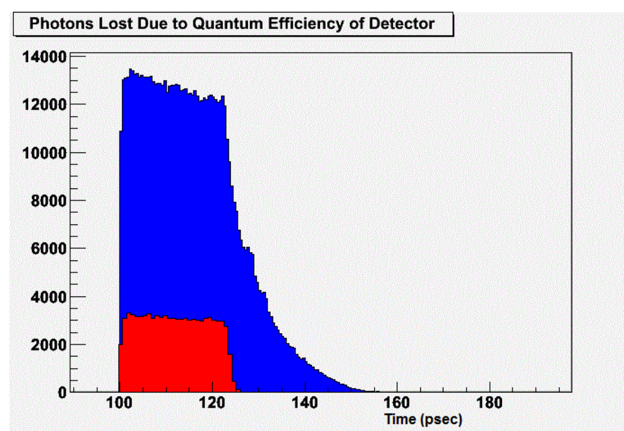

Figure 10: Number of photons arriving at detector versus time (in blue) and number of photoelectrons produced in photodetector versus time (in red).

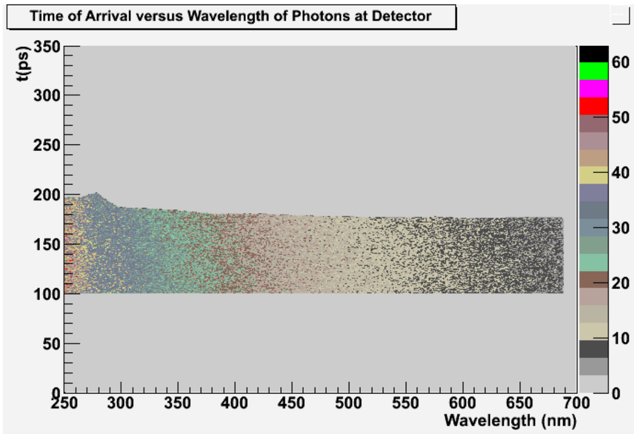

Figure 11: Arrival time of photons incident upon the detector plotted against wavelength.

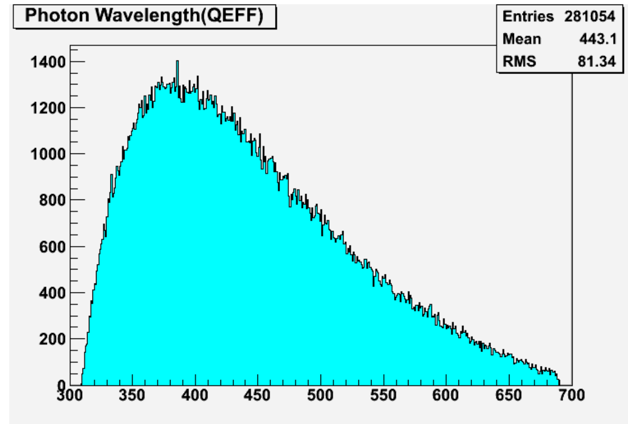

Figure 12: Wavelength distribution of photoelectrons for SiPM.

The MCP has a detection efficiency (the probability of detecting a photon incident upon the detector) for visible light shown in Figure 6. The MPPC has a detector efficiency shown in Figure 5 plotted against wavelength. The number of photoelectrons produced as a function of time is shown in Figure 10, while the number of photoelectrons produced per wavelength is shown in Figure 12, and Figure 13 shows the fraction of photons that produce photoelectrons as a function of wavelength. Combining these two graphs in Figure 14, it is apparent that most of the detected photons are in the 300-450 nm wavelength range. All of these figures were produced for 1 000 proton runs using the SiPM detector.

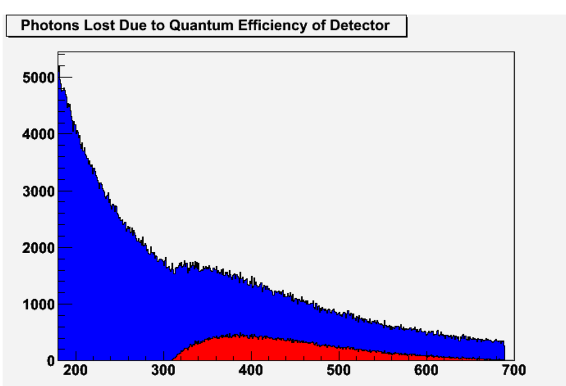

Figure 13: Fraction of photons reaching detector (blue) that produce photoelectrons (red).

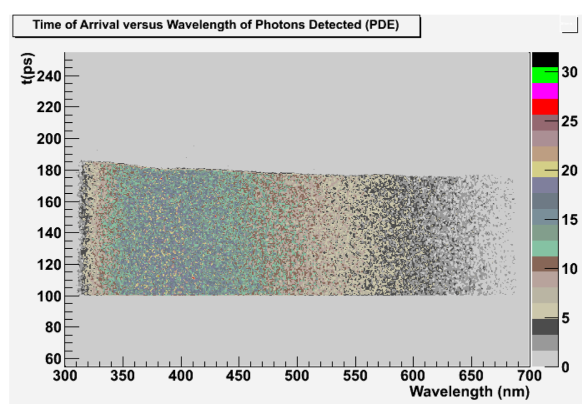

Figure 14: Time of photoelectron production plotted against wavelength of photoelectrons.

The number o photoelectrons produced per event is shown as the red line in Figure 15. The numbr of photons incident upon the detector per event is represented by the green line, as a functin of the length of the quartz radiator bar. Figure 15 also displays the number of photolectrons produced after introducing a constant photon loss factor (0.15) to simulate the numbr of photoelectrons experimentally measured, represented by the blue line. As bar length increaes, so does the number of photons reaching the detector, as well as the number of photons contriuting to the timing signal, in a fairly linear fashion.

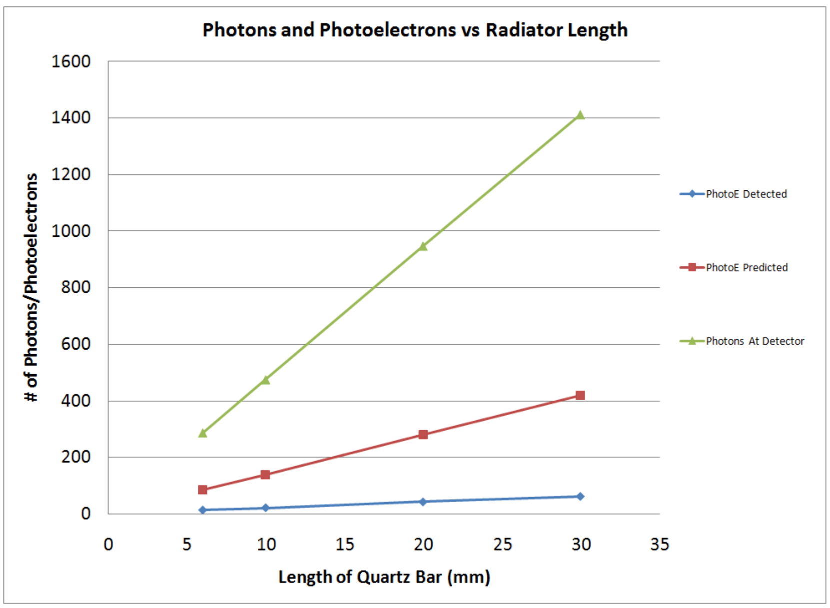

Figure 15: Photons reaching the photodetector (in green), photoelectrons predicted by simulation (in red), and photoelectron production altered by a constant factor of 0.15 to replicate beamline data (in blue) as a function of radiator length.

In Figure 16 we see timing resolutions for the SiPM setup with varying fractions used for the constant fraction discriminator, lengths of radiator, and type of detector. We find that as the constant fraction is increased in the SiPM setup, timing resolution increases, as well as when the quartz bar increases in length in Figure 17. In Figure 18, we find that the timing resolution for the QUARTIC setup gets worse as the quartz bar increases in length, but does not seem to be directly correlated to changes in the fraction at which the CFD is set.

Fraction	0.1	0.1	0.2	0.2	0.4
Protons	1000	1000	1000	1000	1000
Detector	SiPM	MCP	SiPM	MCP	MCP
Timing (psec) 6mm (SiPM/MCP)	4.511	0.6634	4.017	0.6391	0.6773
Timing (psec) 10mm (SiPM/MCP)	2.819	0.906	3.251	0.8933	0.8949
Timing (psec) 20mm (SiPM/MCP)	3.003	1.396	2.745	1.382	1.388
Timing (psec) 30mm (SiPM/MCP)	2.377	1.783	2.296	1.773	1.793

Figure 16: Timing resolutions simulated for SiPM setup using different CFD thresholds, radiator lengths, and detectors.

Fraction	0.1	0.2	0.4
Protons	1000	1000	1000
Timing (psec) 6mm	12.3	10.7	9.4
Timing (psec) 10mm	10.2	9.2	7.7
Timing (psec) 20mm	7.6	6.9	6.1
Timing (psec) 30mm	6.7	6.3	6.0

Figure 17: Timing resolutions using laboratory photoelectron values.

Fraction	0.2	0.4
Protons	1000	1000
Timing (psec) 10mm	13.3	12.2
Timing (psec) 150mm	53.7	55.3

Figure 18: QUARTIC timing resolutions using reduced photoelectron count.

Finally, Figure 19 shows the measured transmission of the quartz bar and lead fluoride crystal.

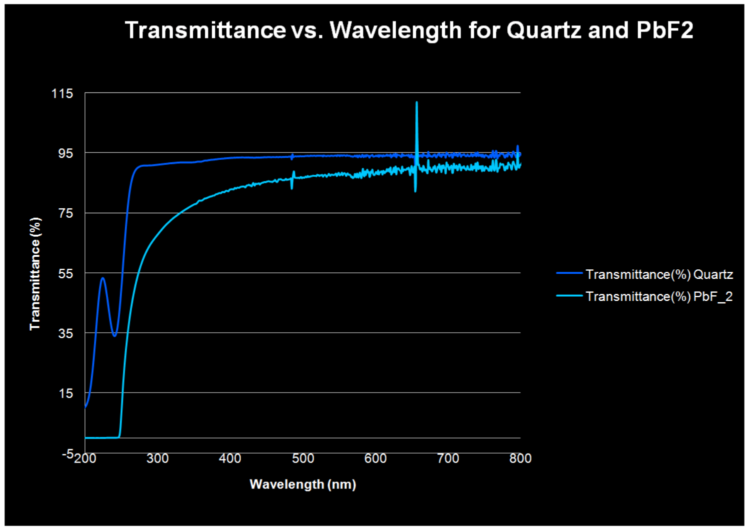

Figure 19: Measured transmittance of quartz crystal and lead fluoride.

DISCUSSION/CONCLUSION

The photon statistics at the end of the detector agree with the expected values. The Cherenkov radiation is mostly in the blue-UV region, and since Cherenkov production is uniform, the photons produced increase linearly with bar length while retaining the same wavelength distribution. UV-blue wavelength photons are also delayed as expected due to dispersion. Thus Geant4 is correctly modeling the radiator.

The plots of the detected photons versus wavelength show the ROOT-generated photodetector is detecting the photons in the manner reported by the photodetector manufacturers. However, when we compare the number of photoelectrons produced in the simulation to the number of photoelectrons detected by the detectors in beam line experiments, we find a discrepancy. The simulation predicts approximately six to seven times the number of photoelectrons detected. This may be caused by edge effects not included in the simulation such as a non-reflective coating on the photodetector, and interactions of the photons with the optical grease that attaches the radiator to the photodetector. An experimental investigation would be extremely useful in determining which of these processes is most likely the cause of the discrepancy, along with an extension of the simulation to model these processes.

Regardless of the cause of this loss of photoelectrons, the simulation produced the same number of photoelectrons as was measured when a fudge factor was introduced to the code, multiplying the quantum efficiency of the detectors by a factor of 0.15. This factor increased the timing resolution, leaving it at approximately half of the experimental value. Further simulations are recommended for understanding the cause of this factor of two difference in the timing resolution values. The primary concern is that in simulating the jitter of the peak for the SiPM, the photoelectron number was artificially increased, which will be investigated shortly. For the MCP, the first photon spread was not taken into account in the measurement, and could account for the timing resolution discrepancy for this detector.

The effects of increasing the fraction at which the CFD is set are probably a result of assuming a Gaussian pulse, which is not the correct pulse shape for a SiPM, and not including noise.

Thus, there are many recommended extensions of this simulation that must be done to make sense of the results that it produced. These further studies will help to augment our understanding of how Cherenkov detectors function, and thus which methods would lead to the most functional optimization of these fast timing detectors.

ACKNOWLEDGEMENTS

I would like to thank the Department of Energy, Office of Science and the Science Undergraduate Laboratory Internships (SULI) program for making this internship possible, and Fermi National Accelerator Laboratory for hosting my internship. I would also like to thank my mentor, Mike Albrow, as well as Hans Wenzel, Earle Wilson, Anatoly Ronzhin and Adam Para for their patience, advice and guidance.

REFERENCES

[1] M.G. Albrow et al. “The FP420 R&D project: Higgs and new physics with forward protons at the LHC,” *Journal of Instrumentation*, vol. 4 issue 10, T10001, October 2009.

[2] D. d’Enteria, “Higgs and beyond the Standard Model physics with the FP420 detector at the LHC,” arXiv:0905.4307 [hep-ex].

[3] M.G. Albrow et al., “Tests of an edgeless quartz timing Cherenkov detector,” *Journal of Instrumentation*, in preparation, results of Fermilab May 2010 test.